SA–CME Information

Imaging Brachial Plexus Pathology

Description

Brachial plexus disorders are a diagnostic challenge due to the complex anatomy and nonspecific symptomatology. MRI remains the best modality for assessing the brachial plexus (BP), due to its superior soft-tissue contrast compared to CT or ultrasound. Traumatic lesions are the most common cause of BP dysfunction, closely followed by neoplastic infiltration. Infection, inflammation and iatrogenic causes are less common.

This review article will provide an overview of anatomy and practical, up-to-date BP imaging techniques for general radiologists, followed by a step-wise discussion of common pathology. Clinically relevant advances such as dynamic thoracic outlet MRI will also be discussed.

Learning Objectives

After completing this activity, the participant will be able to:

- Explain the important role of MRI in the diagnosis of brachial plexus pathology,
- Identify the major pathologies of the brachial plexus including post-traumatic lesions, neoplastic infiltration and infection/inflammation, and,
- Use provocative MRI and ultrasound techniques in the evaluation of thoracic outlet syndrome.

Accreditation/Designation Statement

The Institute for Advanced Medical Education is accredited by the Accreditation Council for Continuing Medical Education (ACCME) to provide continuing medical education for physicians.

The Institute for Advanced Medical Education designates this journal-based CME activity for a maximum of 1 AMA PRA Category 1 Credit™ . Physicians should only claim credit commensurate with the extent of their participation in the activity.

These credits qualify as SA-CME credits.

Authors

James Thomas Patrick Decourcy Hallinan, MBChB, is a Radiologist with the National University Health System, Singapore, and an Assistant Professor of Radiology at the Yong Loo Lin School of Medicine, Singapore; Mini N. Pathria, MD, and Brady K. Huang, MD, are Radiologists with the UC San Diego Health System. Dr. Pathria is a Professor, and Dr. Huang is an Associate Professor of Radiology at the San Diego Medical Center, University of California, San Diego, CA. None of the authors have conflicts of interest to declare..

Target Audience

- Radiologists
- Related Imaging Professionals

System Requirements

In order to complete this program, you must have a computer with a recently updated browser and a printer. For assistance accessing this course online or printing a certificate, email *CustomerService@AppliedRadiology.org*.

Instructions

This activity is designed to be completed within the designated time period. To successfully earn credit, participants must complete the activity during the valid credit period. To receive SA–CME credit, you must:

1. Review this article in its entirety.
2. Visit *www.appliedradiology.org/SAM2*.
3. Login to your account or (new users) create an account.
4. Complete the post test and review the discussion and references.
5. Complete the evaluation.
6. Print your certificate.

Estimated time for completion: **1 hour**
Date of release and review: **November 1, 2019**
Expiration date: **October 31, 2021**

Disclosures

No authors, faculty, or any individuals at IAME or *Applied Radiology* who had control over the content of this program have any relationships with commercial supporters.

Imaging Brachial Plexus Pathology

James Thomas Patrick Decourcy Hallinan, MBChB; Mini N. Pathria, MD; and Brady K. Huang, MD

Brachial plexus disorders can be diagnostic challenges, owing to the region's complex anatomy and nonspecific symptomatology. MRI remains the best modality for assessing the brachial plexus (BP), due to its superior soft-tissue contrast compared to CT or ultrasound. Trauma is the most common cause of BP dysfunction, closely followed by tumor infiltration. Infection, inflammation and iatrogenic causes are less common. This review article will provide an overview of anatomy and practical, up-to-date BP imaging techniques for general radiologists, followed by a step-wise discussion of common pathology. Clinically relevant advances such as dynamic thoracic outlet MRI will also be discussed.

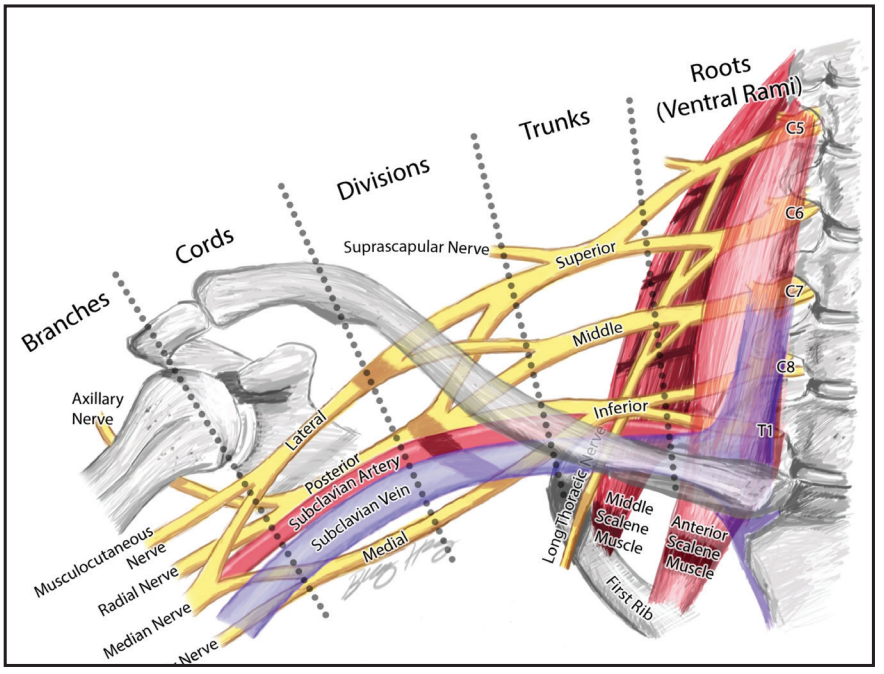

FIGURE 1. *Schematic drawing showing the major components of the brachial plexus. Some of the smaller nerves that arise from the brachial plexus have been omitted, as they are difficult to visualize on routine MRI. Note the relationship of the nerves relative to the muscles, vessels, and osseous structures.*

Anatomy

The BP provides motor innervation to the ipsilateral chest, shoulder, and upper limb with the exception of the trapezius, which is supplied by the spinal accessory nerve. It is divided anatomically into roots, trunks, divisions, cords, terminal and collateral branches (Figure 1). These constituents may best be recalled using this mnemonic: Radiology (roots) Technicians (trunks) Drink (divisions) Cold (cords) Brew (terminal branches) Coffee (collateral branches)—a slight divergence from the usual alcohol-based memory tools.

The BP roots arise from the C5-T1 ventral rami of the spinal cord, with variable C4 and T1 contributions. As a result, the "roots" are actually the ventral rami of the spinal nerves formed from the dorsal and ventral rootlets arising from the spinal cord.[1] Although "roots" is a misnomer, the term is well established in the literature and will be used throughout this article.

The roots exit through their respective neural foramina, and travel between the anterior and middle/posterior scalene muscles in the interscalene triangle,

Dr. Hallinan is a Radiologist with the National University Health System, Singapore, and an Assistant Professor of Radiology at the Yong Loo Lin School of Medicine, Singapore; Dr. Pathria and Dr. Huang are Radiologists with the UC San Diego Health System. Dr. Pathria is a Professor, and Dr. Huang is an Associate Professor of Radiology at the San Diego Medical Center, University of California, San Diego, CA. None of the authors have conflicts of interest to declare.

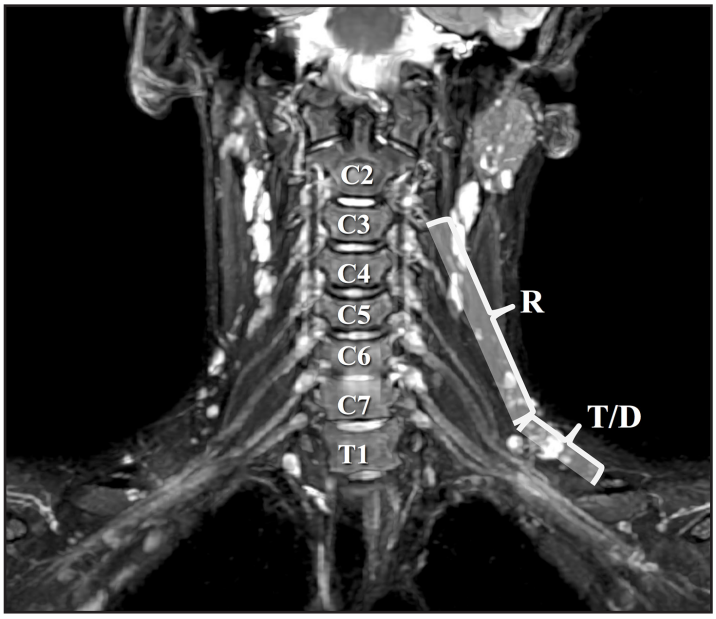

FIGURE 2. *Normal anatomy of the brachial plexus. Coronal T2W IDEAL (fat-saturated) MIP sequence. The brachial plexus roots (R) are well-demonstrated, exiting above their respective vertebral bodies; eg C5 exits at C4-5. The roots travel obliquely in an inferolateral direction to form the trunks and divisions (T/D). IDEAL- Iterative decomposition of water and fat with echo asymmetry and least-squares estimation, MIP- Maximum intensity projection.*

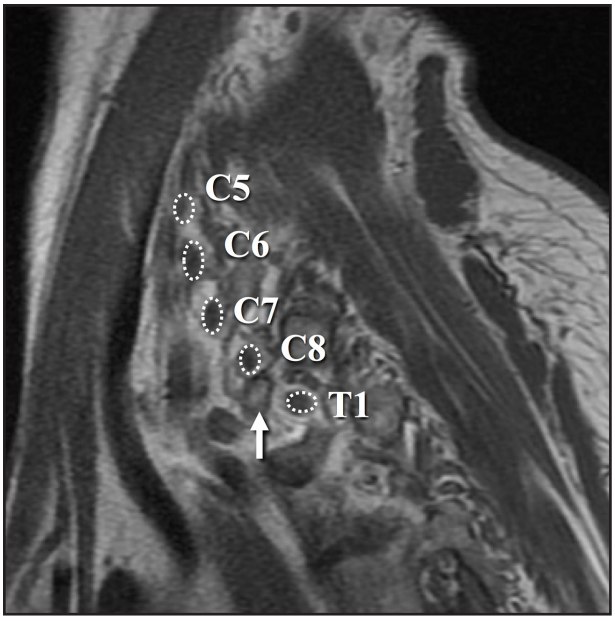

FIGURE 3. *Normal anatomy of the brachial plexus roots. Sagittal T1W image of the brachial plexus at the level of the roots, just lateral to the exit foramina. The first rib (solid arrow) interposes between the C8 and T1 nerve roots.*

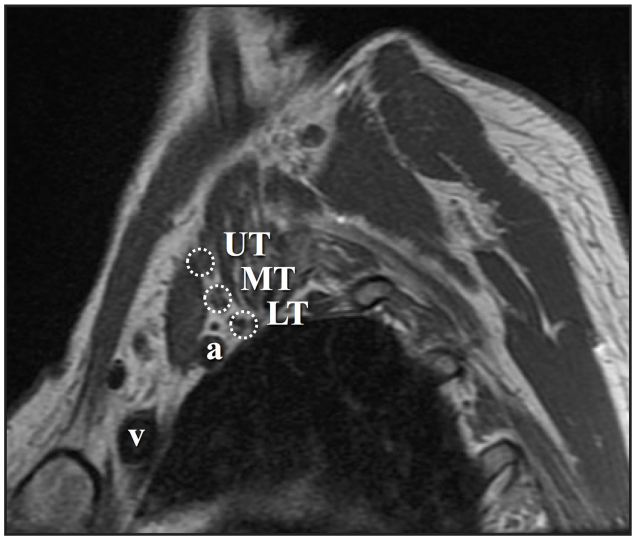

FIGURE 4. *Normal anatomy of the brachial plexus trunks. Sagittal T1W image of the brachial plexus trunks at the interscalene triangle (between the anterior and middle scalene muscles). The subclavian artery (a) is closely related to the lower trunk with the vein (v) located more anteriorly. UT- Upper trunk, MT- Middle trunk, LT- Lower trunk.*

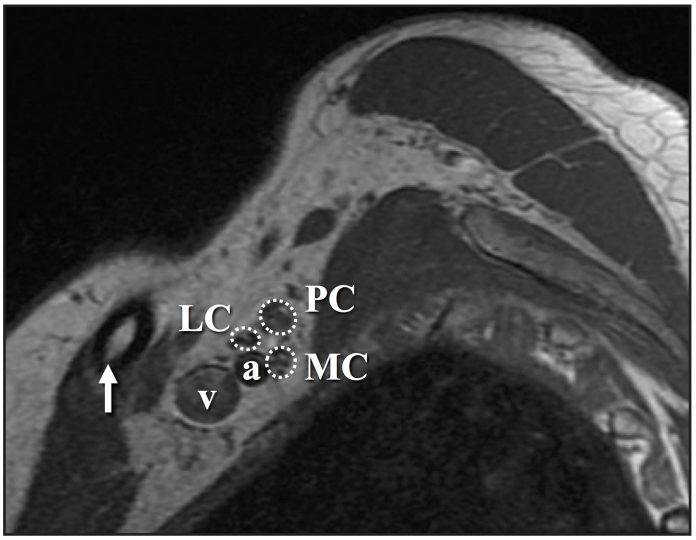

FIGURE 5. *Normal anatomy of the brachial plexus cords. Sagittal T1W image of the brachial plexus cords at the costoclavicular space (clavicle shown by the solid arrow). The subclavian artery (a) is closely related to the lateral and medial cords with the vein (v) located more anteriorly. LC- Lateral cord, MC- Medial cord, PC- Posterior cord.*

or space (Figures 2, 3). Lateral to the middle scalene muscle the three trunks are formed: C5 and C6 combine into the upper trunk, C7 continues alone as the middle trunk, and C8 and T1 combine to form the lower trunk (Figures 2, 4). The trunks traverse posterosuperior to the subclavian artery behind the clavicle and each divides into anterior and posterior divisions within the costoclavicular space. The vessels lie inferiorly at the costoclavicular space with the subclavian vein anterior to the artery.[2,3] This space, bounded by the clavicle superiorly, subclavius muscle anteriorly, and the first rib and middle scalene muscle posteriorly, is a common site of BP and subclavian vascular compression.

The conversion of the six divisions into three cords occurs at the lateral border of the first rib (Figure 5). The cords extend into the retropectoralis minor space and can be readily identified due to their relationship to the axillary artery;

DETAILS ON PAGE 9

Table 1. Innervation of the terminal roots, cords and branches of the BP

Roots	Cords	Branches	Innervates
C5, C6, C7	Lateral	Musculocutaneous	Anterior compartment upper arm
C5, C6	Posterior	Axillary	Deltoid and Teres minor
C5, C6, C7, C8, T1	Posterior	Radial	Posterior compartment of upper and lower arm
C5, C6, C7, C8, T1	Medial and Lateral	Median	Anterior compartment forearm
C7, C8, T1	Medial	Ulnar	Intrinsic hand muscles

Table 2. 3T GE protocol at our institution

MRI sequence	FOV (cm)	Slice thickness (mm)	TR/TE (ms)	Matrix
3D* T1 coronal Cube bilateral	34-38	1.2	650/16.7	320 x 320
3D T2 coronal IDEAL bilateral	34-38	1.2	6000-6500/60-75 (long sequence 8 min)	320 x 320
3D T2 FS coronal bilateral	34-38	1.6	2500/85	320 x 320
T1 axial bilateral	16-18	3	500-600/9	320 x 192
T2 coronal IDEAL ipsilateral	16-18	3	6000-6500/60-75	224 x 160
T2 sagittal IDEAL ipsilateral	16-18	3	6000-6500/60-75	224 x 160
Additional thoracic outlet (TOS) post IV contrast				
1) TRICKS coronal angiogram post-contrast				
2) Coronal T1 LAVA post-contrast bilateral arms down FOV 34-38 cm, Slice thickness 3mm, TR/TE 6.3/3.1, matrix 300 x 200				
3) Coronal T1 LAVA post-contrast bilateral arms up (same parameters as above)				

IDEAL = Iterative Decomposition of water and fat with Echo Asymmetry and Least-squares estimation. TRICKS = Time Resolved Imaging of Contrast KineticS. LAVA = Liver Acquisition with Volume Acceleration.
*3D sequences can be reformatted in any plane (typically sagittal T1W obtained)

The medial cord lies posteroinferiorly, lateral cord anterosuperiorly and posterior cord posterosuperiorly. The cords divide into five major terminal branches at the lateral border of the pectoralis minor: the median, ulnar, radial, musculocutaneous and axillary nerves.[4,5] In addition there are numerous (~11) collateral branches that exit along the BP more proximally, eg,, suprascapular nerve from the superior trunk. Table 1 shows the innervation of the cords and terminal branches.

MR imaging protocol

Accurate visualization of the BP from the roots to terminal branches must take into consideration its oblique superomedial to inferolateral course. As such, oblique coronal and sagittal images are preferred, but not mandatory. Our protocol utilizes initial large field of view images for bilateral comparison of the brachial plexuses. These are typically performed with T1W fast spin echo images and three-dimensional T2W fat-suppressed sequences, which allows for multiplanar reconstructions. In a high-volume facility, isotropic imaging can shorten imaging time and decrease the need for custom-tailored exams.[4,6]

Dedicated, multiplanar, small field of view images of the affected plexus are then performed. Coronal T2W fat-saturated sequences are useful for assessment of abnormal neural edema and enlargement; T1W sagittal images are especially useful for assessment of fat planes along with surrounding bony and muscular anomalies; eg, cervical ribs. [7] High resolution, axial, pre-ganglionic, T2W images of the cervical region and nerve roots are also performed. These are useful for assessment of traumatic nerve root avulsions and pseudomeningoceles.[3,5]

Both 1.5T and 3T platforms may be used, with a sample protocol shown in Table 2 (For 3T only). 3T is preferred due to better resolution and signal-to-noise profile over 1.5T, with 1.5T reserved for patients with hardware or contraindications to 3T. Neurovascular surface coils or a wrap-around body coil can be utilized.

Intravenous gadolinium-based contrast is not routinely required for BP imaging as most nerve pathology is well assessed on the high-resolution, fat-suppressed T2W images. Contrast administration is typically required in cases of suspected infection or tumor infiltration. Contrast allows for more accurate assessment of disease extent, identification of drainable collections and characterization of focal masses, such as neurogenic tumors.[1,4]

Another common indication for imaging is thoracic outlet syndrome (TOS). The aim is to assess for the site of vascular and/or neural compression, which is typically at the costoclavicular space and may involve anomalous ribs

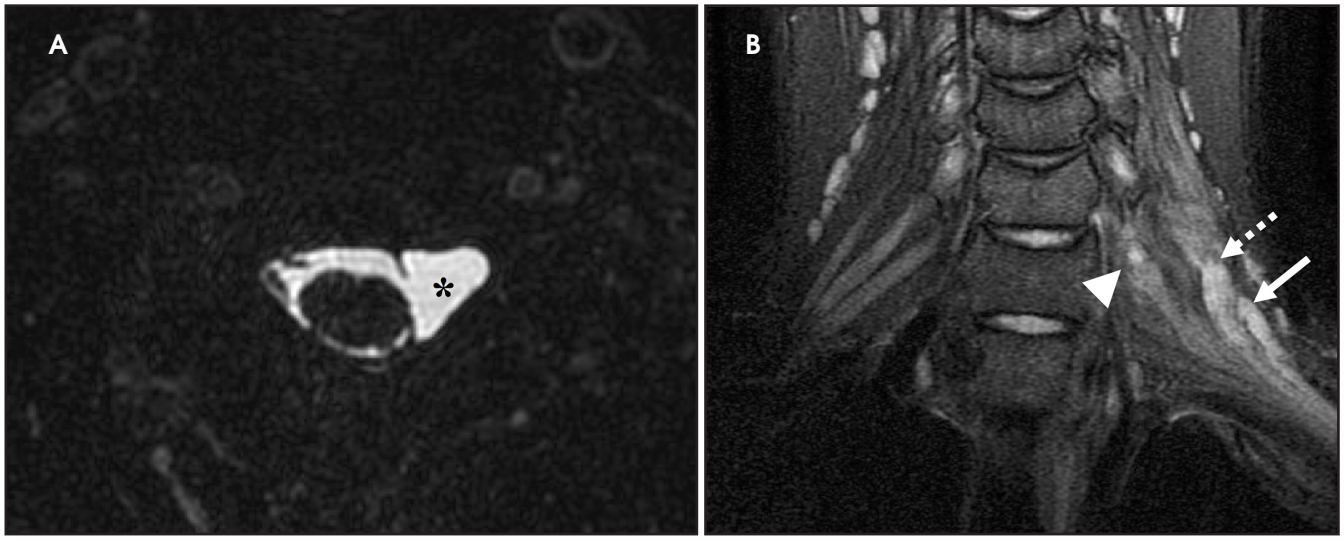

FIGURE 6. *Brachial plexus traumatic preganglionic avulsions in a 20-year-old man with left-sided brachial plexus injury following a bicycle accident. High-resolution, axial T2W, fat-saturated MRI (A) shows a large, left pseudomeningocele (*) at C5-6, which extends from C5 to C7 (not shown), with complete avulsion of the left ventral and dorsal C6 rootlets (normal rootlets are seen on the right side). Coronal, T2W, fat-saturated MRI (B) shows avulsion and distal retraction of the left C5 (solid arrow) and C6 (dashed arrow) nerve roots, with stretching and partial disruption of the left C7 nerve root (arrowhead). There is extensive edema within the trunks and divisions of the left brachial plexus. The normal right-sided brachial plexus roots can be seen for comparison.*

or musculature, or fibrous bands.[4,8] Provocative maneuvers, such as arm raising and head turning, can unmask the extent and location of the compression. Bilateral coronal T1W sequences and post-contrast MR angiography are commonly performed in each position (Table 2).

Diffusion tensor imaging (DTI) with fiber tractography has the potential to detect microstructural abnormalities beyond the resolution of conventional, anatomic MRI sequences. It is still an experimental tool, but has been shown to detect tract disruption, infiltration and internal disorganization, which could allow for earlier diagnosis of neoplastic or inflammatory neuropathies.[5,9,10]

CT of the brachial plexus

CT also plays a role in the diagnosis of BP pathology. Extension of neoplastic disease into the plexus (eg, Pancoast tumor), rib and clavicle anomalies, and adjacent fractures and hematomas can be visualized. CT angiography also provides a high-resolution and rapid assessment of arterial and venous patency in trauma and TOS.

Ultrasound of the brachial plexus

Ultrasound of the BP is technically feasible, but challenging due to the complex anatomy and bony relations.[11,12] In skilled hands, it is a useful bedside tool for assessing traumatic BP injury and is routinely used by anesthesiologists to perform nerve blocks.[13] It is also commonly used for dynamic vascular assessment in suspected TOS.[14,15] Lapeque et al (2014) provide a practical review on BP ultrasound. However, for the majority of BP injuries, MRI remains the standard examination, with ultrasound as a useful adjunct.

Brachial plexus lesions

BP lesions can be classified broadly into two categories: traumatic and non-traumatic lesions.[16] Traumatic lesions form the majority of BP injuries, and are the major indication for imaging. Non-traumatic lesions are a heterogeneous group encompassing neoplastic processes, infection/inflammation and functional neurovascular compression or TOS.[17]

Trauma

Motor vehicle accidents are responsible for the majority of traumatic BP injuries. Traumatic traction on the BP can lead to proximal spinal nerve root avulsion (pre-ganglionic) or more distal rupture (post-ganglionic).[18]

Clinical examination of the neurological injury should be documented promptly to determine the site and clinical course of lesions (recovery or stable deficit) and whether surgery is indicated. Upper limb paralysis is complete in approximately 75% of patients, with a supraclavicular site of injury seen in 72% of cases.[19] Delineation of the site of injury is important for prognosis and management. Pre-ganglionic injuries may require early (<3 months) reconstruction using nerve transfers, whereas postganglionic injuries may be repaired after a longer period of observation.[1,5]

Identification of pre-ganglionic lesions requires high-resolution 3D T2W images, which are typically viewed in the axial plane (Figure 6). Intradural nerve rootlets should be assessed for integrity from the root entry zone to the dorsal root ganglion within the neural foramen. These injuries are associated with traumatic pseudomeningoceles in 80% of cases.[1,5,12] Other common associated findings in pre-ganglionic avulsion include contralateral cord displacement, syrinx, epidural hematoma and spinal cord edema. The posterior paraspinal musculature should also be assessed for denervation edema, which can occur due to a nerve root avulsion

DETAILS ON PAGE 9

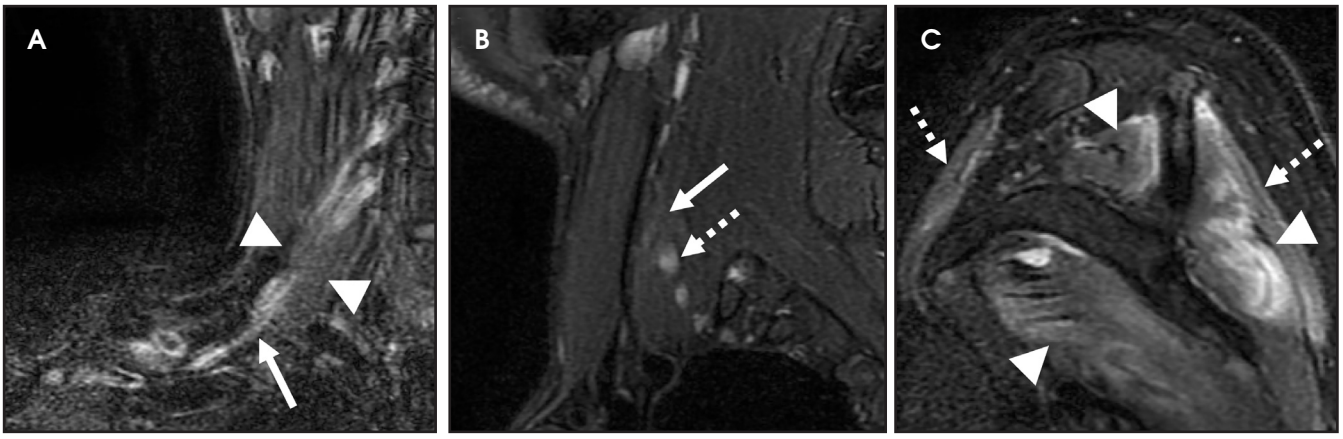

FIGURE 7. *Brachial plexus traumatic postganglionic avulsions in a 39-year-old man following a motorcycle accident. Coronal T2W, fat-saturated MRI (A) of the right brachial plexus shows apparent discontinuity of the postganglionic C5 and C6 nerve roots (between the arrowheads). There is extensive downstream edema within the upper trunk of the right brachial plexus (solid arrow). On sagittal T2W, fat-saturated MRI sequences (B-medial and C-lateral at the shoulder girdle) there is an absence of the C5 nerve root at the expected position compatible with complete avulsion (solid arrow in B), with diffuse enlargement of the C6 nerve root, likely due to severe stretching (dashed arrow in B). Associated denervation edema and atrophy of the right shoulder girdle musculature, including the rotator cuff muscles (arrowheads in C) and deltoid muscle (dashed arrows in C), are seen.*

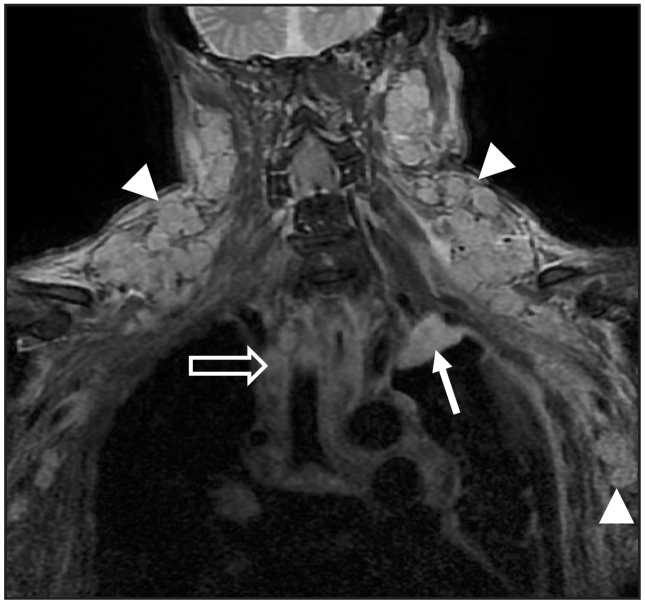

FIGURE 8. *Nodal metastases with extracapsular extension at the brachial plexuses in a 67-year-old man with known thyroid carcinoma. Coronal, contrast-enhanced, T1W, fat-saturated MRI sequence shows numerous, enhancing, bilateral nodal metastases (arrowheads) with extensive involvement of the brachial plexuses and axillary regions (best seen on the left). There are additional pleural metastases at the left lung apex (solid arrow) with mediastinal lymphadenopathy (open arrow).*

FIGURE 9. *Pancoast (superior sulcus) tumor with invasion of the brachial plexus in a 43-year-old man. Coronal T2W, fat-saturated MRI shows a Pancoast tumor at the left lung apex (solid arrow) with extension into the lower neck and involvement of the mid to lower roots (mainly C6-T1) and trunks of the brachial plexus (dashed arrows). There was additional encasement of the left subclavian artery and vein (not shown), which along with the extensive neural involvement, precludes surgical resection.*

at or before the dorsal root ganglion. Stretching or incomplete avulsion of the pre-ganglionic rootlets is more challenging to diagnose, and may be suggested when there is differential enhancement of the rootlets.[1,5]

Post-ganglionic avulsions distal to the neural foramina typically occur proximally at the scalene triangle, but may variably involve the trunks to distal branches. These can also be partial or complete; complete ruptures are usually associated with distal nerve retraction (Figure 7). Another finding is nodular thickening and mild enhancement due to a post-traumatic neuroma in continuity. Indirect findings include formation of hematomas at the site of avulsion and denervation edema and enhancement at the shoulder girdle musculature.[1,5,20]

MRI is the mainstay for diagnosis, although ultrasound can provide an accessible bedside examination in critically injured patients. [11] Ultrasound can be

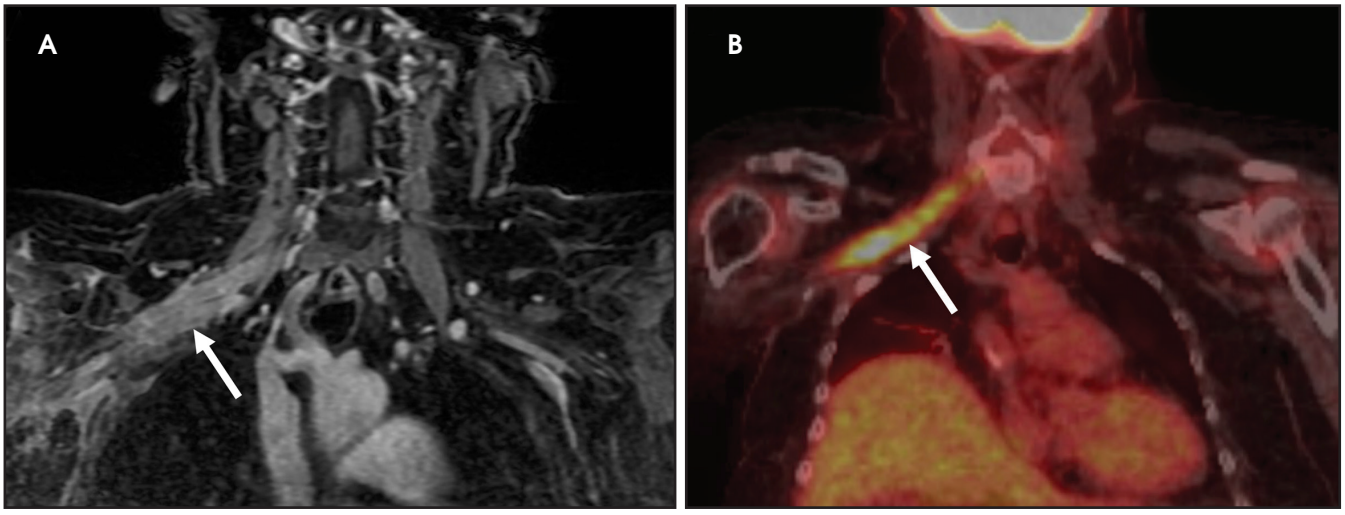

FIGURE 10. *Metastatic versus radiation plexopathy in a 67-year-old woman with metastatic breast carcinoma (known pulmonary metastases). Coronal, contrast-enhanced, T1W, fat-saturated MRI sequence (A). Additional coronal reconstruction from a subsequent FDG-PET/CT (B). There is extensive contrast-enhancement of the right brachial plexus, extending from the trunks to the axillary region (solid arrow). Prior scans had shown less marked aggregation and enhancement, likely in favor of post-radiotherapy plexopathy (images not shown). Due to the interval progression, metastatic disease was a key consideration and an FDG-PET/CT confirmed the presence of avid FDG uptake along the brachial plexus (solid arrow). This was highly suspicious for metastatic disease and a biopsy was confirmatory. In equivocal cases, FDG-PET/CT is a useful tool to distinguish radiation versus metastatic plexopathy.*

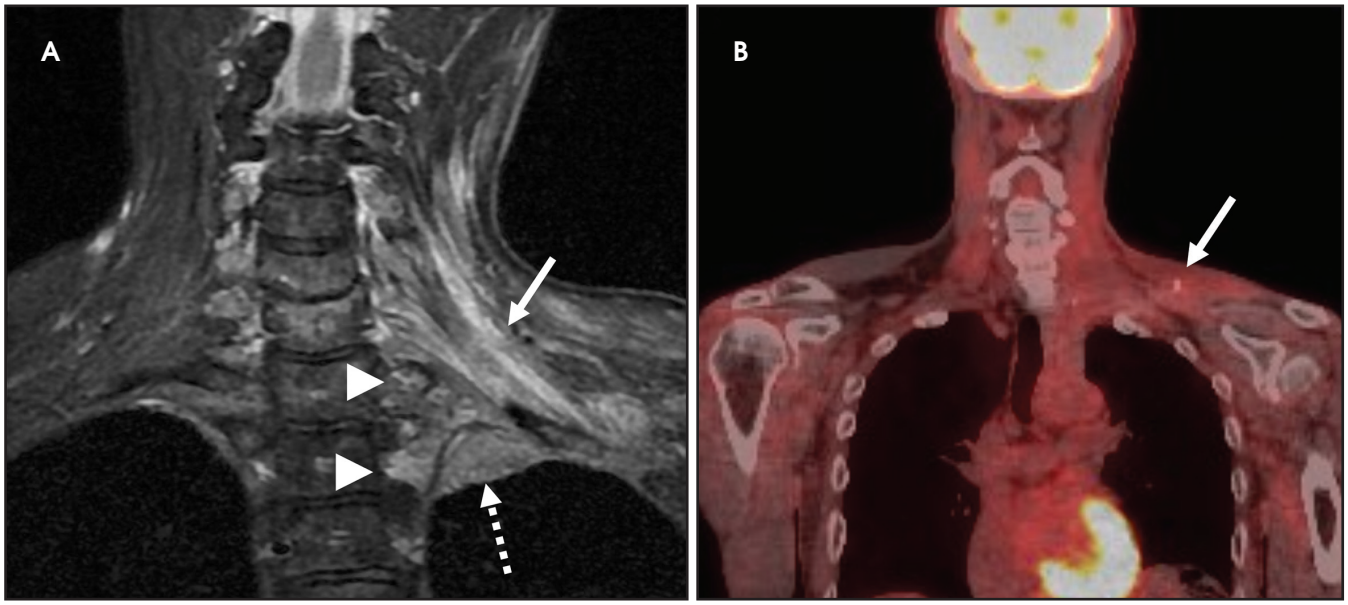

FIGURE 11. *Post-radiation brachial plexopathy in a 53-year-old with metastatic hypopharyngeal squamous cell carcinoma. Coronal, T2W, fat-saturated MRI sequence (A) and a coronal reconstruction from a subsequent FDG-PET/CT (B). There is extensive T2W hyperintense aggregation and thickening of the left brachial plexus (solid arrow in A), involving the roots through to the cords with overlying soft tissue and muscular thickening and edema. There is nodular soft tissue at the left lung apex (dashed arrow) with altered signal at the left first and second ribs (arrowheads in A). Compared to the pre-radiation studies (not shown) the edema and neural thickening showed interval increase in extent with no new focal mass. Along with the paucity of FDG avidity at the left brachial plexus (solid arrow in B) and thoracic inlet on the PET/CT, these findings were compatible with post-radiation plexopathy, left apical fibrosis and post-radiation osteonecrosis of the ribs. Continued surveillance was recommended as this patient remained at high risk of recurrence.*

used to assess for post-ganglionic injuries at the interscalene triangle or distal to the costoclavicular space. Thickening or discontinuity of the trunks or cords can be assessed using the contralateral side as a readily accessible control.[10,11,12] CT myelography also remains an accurate technique for assessing pre-ganglionic avulsions with clear depiction of the intradural rootlets.[17,21]

Plexus traction injuries in neonates are well-recognized, although they are uncommonly imaged. Traction on the superior plexus at C5-7 (Erb-Duchenne palsy) is more common than the inferior plexus at C8 and T1 (Klumpke palsy). These injuries are usually managed conservatively, with surgery reserved

DETAILS ON PAGE 9

FIGURE 12. *Brachial plexus neurogenic tumors in a 47-year-old woman with chronic neck pain and right arm numbness following a motor vehicle accident 2 years ago. Coronal T2W, fat-saturated MRI sequences of the right brachial plexus show two round, T2W hyperintense masses at the right brachial plexus. The dominant mass (solid arrow) involves the cords and branches of the right brachial plexus at the costoclavicular space, with the smaller lesion (dashed arrow) in the retropectoral space in close relation to the proximal branches. Both lesions demonstrate a target sign (better seen at the dominant lesion), with relative central T2W hypointensity. These findings are most compatible with schwannomas or neurofibromas. No surgical intervention is planned at the current time with continued imaging follow-up advised.*

for those with poor functional recovery and suspected pre-ganglionic injury on imaging. [1,22]

Malignant neoplasms

Malignant involvement of the BP is more common than primary benign lesions, and occurs in an older age group. The BP can be infiltrated by primary malignant tumors, local secondary malignancy or metastatic disease (Figure 8). Lesions arising directly from the plexus include malignant peripheral nerve sheath tumors and a plethora of uncommon sarcomatous lesions (eg, fibrosarcoma or radiation induced tumors). Local malignant extension commonly occurs secondary to a Pancoast tumor at the lung apex or due to a head and neck carcinoma (Figure 9). [1,5,15]

These lesions can involve multiple structures including the vertebral bodies, ribs and clavicle with compression and direct invasion of the neural and vascular structures. Clinically, there is usually pain followed by paraesthesia and weakness at the upper limb, predominantly involving the inferior trunk and spinal nerves in a Pancoast tumor. In addition, adjacent infiltration of the sympathetic chain (stellate ganglion) may result in Horner's syndrome.[6,23]

Metastatic disease of the BP commonly arises in the adjacent regional lymph nodes. In particular, breast carcinoma can metastasize along the axillary and supraclavicular nodes resulting in focal masses or even diffuse plexus infiltration (Figure 10). Head and neck carcinomas and lymphoma are other common causes of metastatic infiltration.[16,17]

MR imaging for suspected malignant involvement should include post-contrast sequences to assess for focal masses and any perineural or leptomeningeal enhancement extending to the spinal cord. The imaging report should also document potential involvement of the ipsilateral vertebral artery, which could be further evaluated using MR angiography.[1,5,6]

Radiation plexopathy

Any discussion of malignant infiltration at the BP is incomplete without considering treatment complications. Radiotherapy is utilized for numerous malignancies and secondary nodal disease at the plexus, including breast, lung and head and neck carcinomas. Radiotherapy is a common cause of non-traumatic plexus injury with histology showing fibrous tissue sheathing the plexus and underlying neural degeneration. As in other forms of plexopathy, parasthesias dominate the clinical picture, with motor loss less common.[1,13,17]

On imaging, it is challenging to differentiate radiation plexopathy from recurrent/residual tumor. MRI of radiation plexopathy in the acute phase (<6months) appears as a non-specific plexopathy with diffuse neural thickening, T2W hyperintensity and mild enhancement (Figure 11). In the more chronic fibrotic phase MRI can demonstrate T2W and T1W hypointense thickening without a focal mass. Enhancement is variable in the fibrotic phase, again making differentiation from tumor challenging. [24] Clinical history is crucial to assess for this entity, with information such as radiation dose (less likely if less than 50Gy) and time course (peak presentation is several years after therapy) especially useful. When doubt remains, early follow-up MRI or additional FDG PET-CT, which can assess for recurrent hypermetabolic tumor, can be utilized.[3,25]

FIGURE 13. *Brachial plexus neuritis in a 23-year-old male with poorly controlled diabetes, acute left arm weakness in a C5-6 distribution and worsening recent right lower limb pain and weakness. Coronal (A) and sagittal (B) T2W, fat-saturated (IDEAL) sequences of the brachial plexuses and left shoulder girdle musculature are shown. There is hyperintensity at the C5 and C6 roots and upper trunk (solid arrow in A), which is suggestive of neural edema and inflammation with no discrete mass detected. At the left shoulder girdle there is T2W hyperintensity at the rotator cuff musculature, mainly involving the supraspinatus (arrowhead) and infraspinatus (dashed arrow). These findings are compatible with a brachial plexus neuritis and acute muscle denervation, predominantly involving the distribution of the suprascapular nerve. Given the clinical history these findings could relate to a diabetic polyneuropathy multiplex or Parsonage-Turner syndrome. Unfortunately, the patient was lost to follow-up. IDEAL-Iterative decomposition of water and fat with echo asymmetry and least-squares estimation.*

Benign neoplasms

Numerous benign lesions can arise directly from or in the vicinity of the BP. Peripheral nerve sheath tumors (PNST) such as schwannomas and neurofibromas are the most common primary benign lesion of the BP. [26] The majority of PNST are not associated with underlying neurofibromatosis. Patients usually report a painless supraclavicular mass without parasthesia or weakness. A positive Tinel sign may be present. On imaging the lesions are usually well-circumscribed, ovoid (parallel to the course of the BP), with T2W hyperintensity and avid enhancement. A target sign may also be demonstrated (more commonly in neurofibromas) consisting of central low signal and surrounding peripheral T2W hyperintensity (Figure 12). Schwannomas may also demonstrate the salt and pepper fascicular sign, and can undergo degenerative cystic changes (ancient schwannoma).[1,26]

Other compressive benign lesions arising in the vicinity of the BP include lipomas, fibroproliferative conditions, and vascular lesions (eg hemangioma, arteriovenous malformations or pseudoaneurysms).[24]

Lipomatous lesions are well characterized on both ultrasound and MRI. On T1W and T2W images the lesions are hyperintense with loss of signal on fat suppression. Differentiating lipomas from low-grade liposarcomas remains difficult, although imaging features such as numerous thick septations, extensive non-fatty components and a large size (>10cm) suggest a more malignant potential.[27]

Fibroproliferative conditions can present as large masses and include fibromatosis (locally aggressive extra-abdominal desmoid tumor) and nodular fasciitis. The former is typically painless with MRI demonstrating avid enhancement, heterogeneous T2W and hypointense T1W signal and infiltrative margins. In contrast, nodular fasciitis usually presents as a markedly tender mass with similar MR signal characteristics but less marked enhancement. Surgical resection is typically curative in nodular fasciitis, whereas fibromatosis is prone to recurrence following resection and is therefore difficult to treat. For this reason, close MRI follow-up is common in fibromatosis, and may coincide with additional radiation or chemotherapy.[1,5,17,28]

Brachial plexitis

Inflammation of the BP, termed brachial plexitis, typically presents with acute onset of severe shoulder pain, parasthesias and delayed weakness with muscular atrophy. On clinical follow-up the typical clinical course of pain improvement followed by muscle weakness can differentiate the condition from cervical spondyloarthropathy. The supraspinatus nerve is most commonly affected (~97%) and is involved solely in half of cases.[13,17]

The cause of brachial plexitis remains uncertain with viral, post-vaccination or auto-immune mechanisms postulated. It is therefore usually termed acute sporadic brachial plexitis or Parsonage-Turner syndrome. [8] A subset of brachial plexitis can occur due to autosomal dominant hereditary neuralgic amyotrophy. Another condition

DETAILS ON PAGE 9

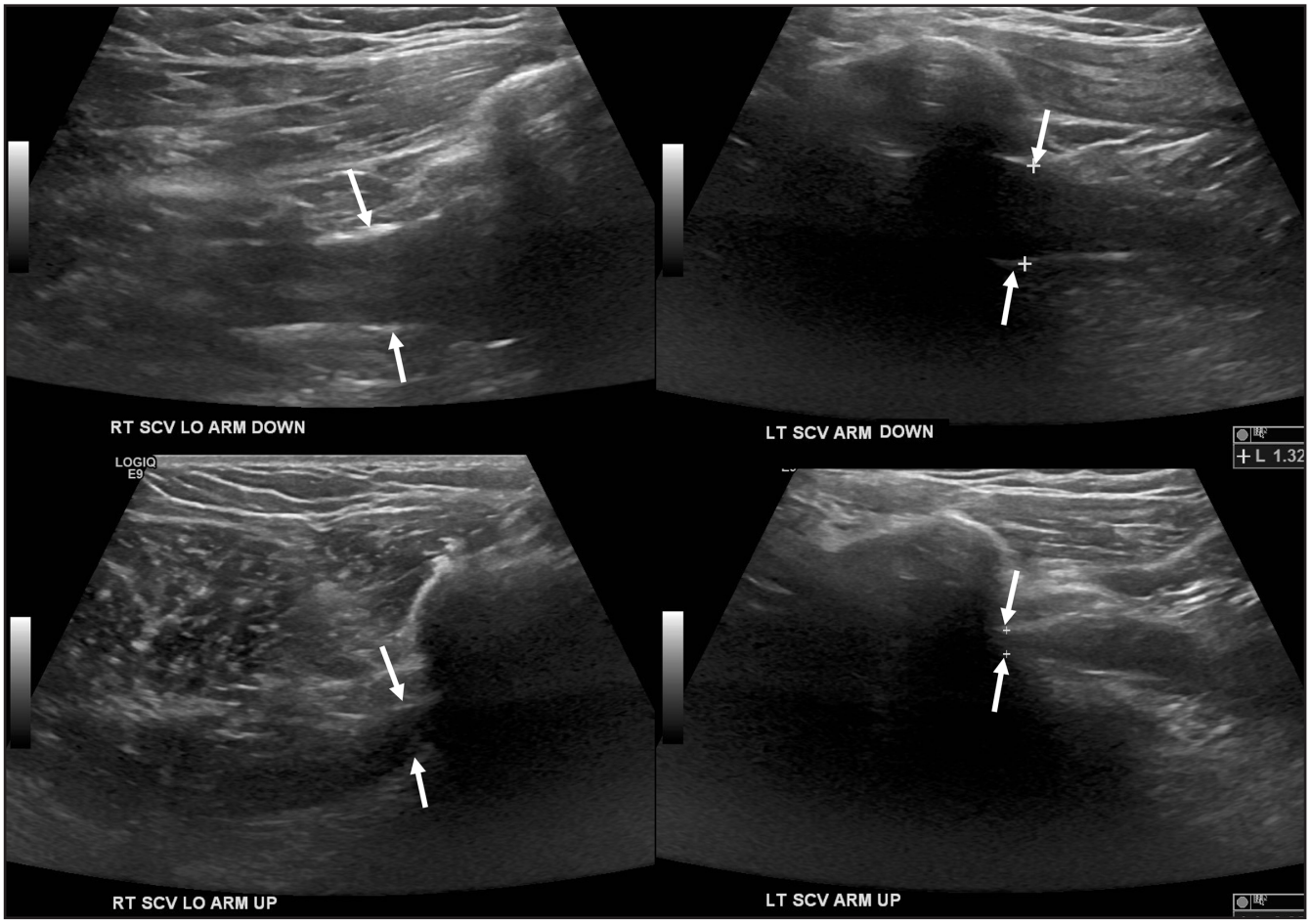

FIGURE 14. *A 30-year-old man with mild neurogenic symptoms (numbness and tingling without weakness) during overhead activities. B-mode ultrasound was performed for suspected bilateral thoracic outlet syndrome with arms up and down as indicated. Dynamic imaging demonstrates narrowing of the subclavian veins upon arm raising at the costoclavicular spaces. These changes are more apparent on the left-side (solid white arrows highlight the caliber of the subclavian veins). This patient did not want to proceed with MRI, which would allow better evaluation of any neural compression or underlying compressive lesion.*

to be aware of is chronic inflammatory demyelinating polyneuropathy, which is rare but classically leads to marked, diffuse thickening of the cervical nerve roots and plexus.[29]

MRI is the preferred examination and in the acute phase may show denervation edema in the shoulder girdle musculature, which can progress to fatty atrophy with chronicity (Figure 13). Less commonly, MRI can show nerve root thickening and edema with increased T2W signal.[17,24] Contrast administration is not strictly required, but can highlight neural enhancement, indicative of ongoing active inflammation. Practically, the major role of MRI is to exclude a compressive mass, which may require surgical intervention. Ultrasound does not have a major role in brachial plexitis, but may highlight fatty atrophy of the shoulder girdle musculature, and can also exclude compressive lesions; eg, a spinoglenoid notch cyst leading to suprascapular nerve compression.[11,13]

Infection

Infection of the BP is uncommon and can occur secondary to penetrating trauma or adjacent soft tissue infection, vertebral osteomyelitis, septic arthritis of the glenohumeral joint or direct extension of infection from the lung apex. In patients with suspected infection, especially the immunocompromised, there should be a low threshold for contrast-enhanced MRI. This allows for assessment of infective extent, any adjacent primary source; eg,spinal infection, and for any fluid collections, which could then be targeted for aspiration or surgical debridement. Numerous pathogens are implicated with bacterial infections most common, especially staphylococcus aureus or tuberculosis.[1,5,30]

Thoracic outlet syndrome

Compression of the subclavian vessels and BP as they traverse the thoracic outlet may produce symptoms such as paresthesia, pain, or swelling. Three potential sites of entrapment exist: interscalene triangle, costoclavicular space (most common site of arterial compression) and the retropectoralis minor space.[8,31] The clinical evaluation of this syndrome is challenging, and provocative ultrasound and MRI can be used in tandem to aid diagnosis. Ultrasound can provide real-time evaluation of vessel stenosis or occlusion

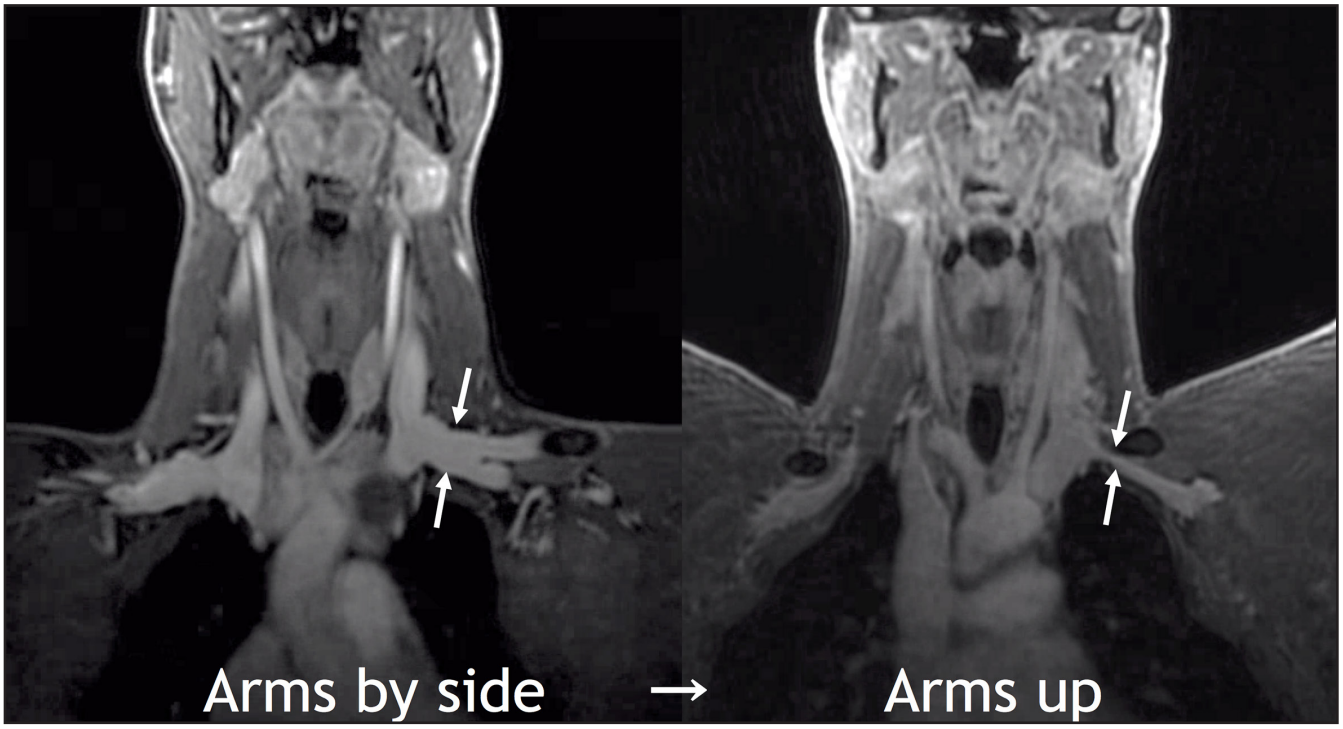

FIGURE 15. *A 19-year-old male with numbness in an ulnar distribution at both hands on arm raising, more marked on the left. Contrast-enhanced MR angiography was performed using Time Resolved Imaging of Contrast KineticS (TRICKS) for suspected thoracic outlet syndrome. Dynamic imaging with arms up and down demonstrates narrowing of the subclavian veins upon arm raising. These changes were more apparent on the left-side with >50% narrowing (solid white arrows). No evidence of neural edema or thickening was seen to suggest neural impingement (images not shown).*

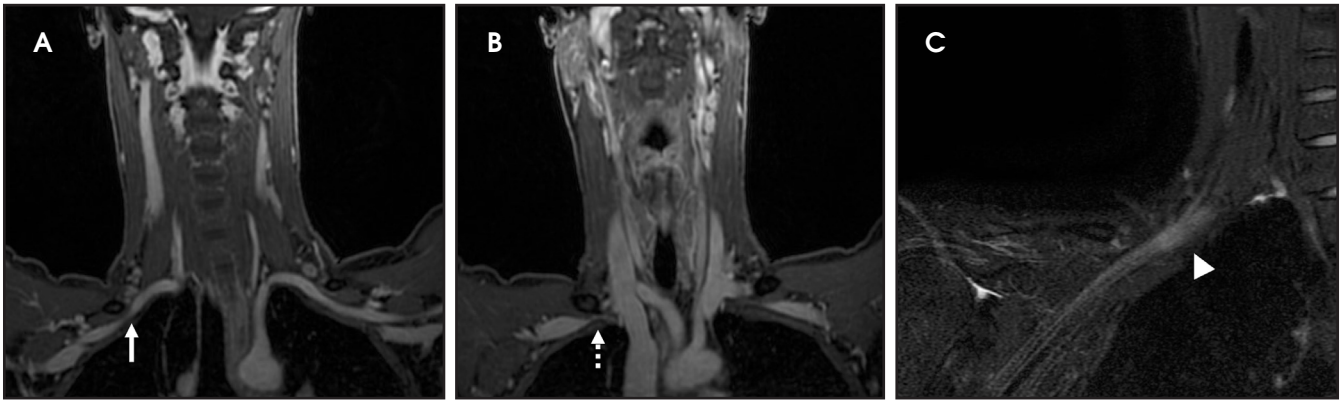

FIGURE 16. *A 30-year-old woman with intermittent right arm swelling and pain. Contrast-enhanced MR angiography (A and B with arms raised) was performed using Time Resolved Imaging of Contrast KineticS (TRICKS) for suspected thoracic outlet syndrome. The arterial phase (A) shows narrowing of the right subclavian artery (solid arrow) at the costoclavicular space. Minimal narrowing of the contralateral left subclavian artery is also apparent. On the venous phase (B) there is narrowing of both subclavian veins, more marked on the right (dashed arrow) in the same region. Coronal T2W, fat-saturated MRI of the right brachial plexus (C) shows additional edema and enlargement of the trunks and proximal divisions of the brachial plexus (arrowhead), again at the costoclavicular space. No enlargement or edema of the nerves was noted on the left-side (images not shown). These findings were compatible with right-sided neurovascular thoracic outlet syndrome. There was an incomplete improvement with physical therapy, so the patient underwent external neurolysis of all the brachial plexus trunks, anterior and middle scalenectomy, and resection of the first rib. After 4 months follow-up there was >70% improvement and the patient resumed athletic activities.*

using B-mode and Doppler imaging (Figure 14). MRI can then provide high-resolution anatomical detail to highlight the site of compression (Figure 15).[8,13]

Provocative maneuvers typically involve arm hyperabduction, which accentuates any narrowing at the costoclavicular and retropectoralis minor spaces. The syndrome may result from a variety of causes including a cervical rib, anomalous muscle (eg, subclavius posticus muscle), clavicular fractures with callus formation, fibrous bands or neoplastic lesions.[1,17,32,33,34] Diagnosis can be challenging as some degree of venous compression is apparent in most asymptomatic patients on arm abduction.[35] In this regard, bilateral imaging may high-

DETAILS ON PAGE 9

light the region of abnormal narrowing on the symptomatic side (Figure 16).

Cervical spondylosis

Due to the vague and non-specific symptoms of BP lesions, it is important to first exclude much more common cervical spondylotic changes. Disc bulges, osteophytes, uncovertebral and facet joint arthropathy can combine to cause cervical cord and/or nerve root compression. Although the cervical spine is covered to some degree on BP protocols, initial dedicated cervical spine MRI may identify the cause of the clinical complaint avoiding the need for the more time intensive BP examination.

Conclusion

The BP can be imaged in detail using dedicated MRI protocols, which allow for accurate interpretation by the radiologist. A dedicated BP protocol should include bilateral coronal and unilateral sagittal sections to identify normal anatomy and highlight pathology. A plethora of lesions occur at the BP, predominantly associated with trauma, but also including primary and secondary neoplasia, inflammation and less commonly infection. Practical reporting should include the site of the BP lesion (pre versus post-ganglionic), involved segment (eg, root, division, etc.), and any associated mass or compressive structure (eg, cervical rib). In the latter, a dedicated thoracic outlet MRI protocol in tandem with Doppler ultrasound can be used to assess dynamic changes in adjacent subclavian vascular caliber and flow.

References

1. Mikityansky I, Zager EL, Yousem DM, et al. MR Imaging of the brachial plexus. *Magn Reson Imaging Clin N Am.* 2012;20(4):791-826.
2. Johnson EO, Vekris M, Demesticha T, et al. Neuroanatomy of the brachial plexus: normal and variant anatomy of its formation. *Surg Radiol Anat.* 2010;32(3):291-297.
3. Castillo M. Imaging the anatomy of the brachial plexus: review and self-assessment module. *AJR Am J Roentgenol.* 2005;185(6 Suppl):S196-204.
4. Lury KM, Castillo M. Imaging of the brachial plexus. *Appl Radiol.* April 13, 2004. https://www.appliedradiology.com/articles/imaging-of-the-brachial-plexus Accessed June 8, 2018
5. Vijayasarathi A, Chokshi FH. MRI of the brachial plexus: A practical review. *Appl Radiol.* 2016;45(4):9-18.
6. Chhabra A, Thawait GK, Soldatos T, et al. High-resolution 3T MR neurography of the brachial plexus and its branches, with emphasis on 3D imaging. *AJNR Am J Neuroradiol.* 2013;34(3):486-497.
7. Torres C, Mailley K, O'Donovan R. MRI of the Brachial Plexus: Modified Imaging Technique Leading to a Better Characterization of Its Anatomy and Pathology. *Neuroradiol J.* 2013; 26(6): 699–719.
8. Linda DD, Harish S, Stewart BG, et al. Multimodality imaging of peripheral neuropathies of the upper limb and brachial plexus. *Radiographics.* 2010;30(5):1373-1400.
9. Tagliafico A, Calabrese M, Puntoni M, et al. Brachial plexus MR imaging: accuracy and reproducibility of DTI-derived measurements and fibre tractography at 3.0-T. *Eur Radiol.* 2011;21(8):1764-1771.
10. Martín Noguerol T, Barousse R, Socolovsky M, et al. Quantitative magnetic resonance (MR) neurography for evaluation of peripheral nerves and plexus injuries. *Quant Imaging Med Surg.* 2017;7(4):398-421.
11. Haber HP, Sinis N, Haerle M, et al. Sonography of brachial plexus traction injuries. *AJR Am J Roentgenol.* 2006;186(6):1787-1791.
12. Graif M, Martinoli C, Rochkind S, et al. Sonographic evaluation of brachial plexus pathology. *Eur Radiol.* 2004;14(2):193-200.
13. Lapegue F, Faruch-Bilfeld M, Demondion X, et al. Ultrasonography of the brachial plexus, normal appearance and practical applications. *Diagn Interv Imaging.* 2014;95(3):259-275.
14. Haun DW, Cho JC, Clark TB, et al. Normative cross-sectional area of the brachial plexus and subclavian artery using ultrasonography. *J Manipulative Physiol Ther.* 2009;32(7):564-570.
15. Demondion X, Vidal C, Herbinet P, et al. Ultrasonographic assessment of arterial cross-sectional area in the thoracic outlet on postural maneuvers measured with power Doppler ultrasonography in both asymptomatic and symptomatic populations. *J Ultrasound Med.* 2006;25(2):217-224.
16. Posniak HV, Olson MC, Dudiak CM, et al. MR imaging of the brachial plexus. *AJR Am J Roentgenol.* 1993;161(2):373-379.
17. Panwar JS, Jakkani RK, Thomas BP. TMR Imaging of non-traumatic intrinsic brachial plexus neuropathy: Spectrum of findings. *J Nucl Med Radiat Ther.* 2015;6(5):246-255.
18. Yoshikawa T, Hayashi N, Yamamoto S, et al. Brachial plexus injury: clinical manifestations, conventional imaging findings, and the latest imaging techniques. *Radiographics.* 2006;26(Suppl 1):S133-143.
19. Silbermann-Hoffman O, Teboul F. Post-traumatic brachial plexus MRI in practice. *Diagn Interv Imaging.* 2013;94(10):925-943.
20. Kim DH, Murovic JA, Tiel RL, et al. Infraclavicular brachial plexus stretch injury. *Neurosurg Focus.* 2004;16(5):1-6.
21. Nagano A, Ochiai N, Sugioka H, et al. Usefulness of myelography in brachial plexus injuries. *J Bone Joint Surg.* 1989;14:59-64.
22. Hale HB, Bae DS, Waters PM. Current concepts in the management of brachial plexus birth palsy. *J Hand Surg Am.* 2010;35(2):322-331.
23. Lee JH, Cheng KL, Choi YJ, et al. High-resolution imaging of neural anatomy and Pathology of the Neck. *Korean J Radiol.* 2017;18(1):180-193.
24. Boulanger X, Ledoux JB, Brun AL, et al. Imaging of the non-traumatic brachial plexus. *Diagn Interv Imaging.* 2013;94(10):945-956.
25. Pierce SM, Recht A, Lingos TI, et al. Long-term radiation complications following conservative surgery (CS) and radiation therapy (RT) in patients with early stage breast cancer. *Int J Radiat Oncol Biol Phys.* 1992;23(5):915–923.
26. Saifuddin A. Imaging tumours of the brachial plexus. *Skeletal Radiol.* 2003;32(7):375–387.
27. Kransdorf MJ, Bancroft LW, Peterson JJ, et al. Imaging of fatty tumors: distinction of lipoma and well-differentiated liposarcoma. *Radiology.* 2002;224(1):99–104.
28. Skubitz KM. Biology and treatment of aggressive fibromatosis or desmoid tumor. *Mayo Clin Proc.* 2017;92(6):947-964.
29. Lozeron P, Lacour MC, Vandendries C, et al. Contribution of plexus MRI in the diagnosis of atypical chronic inflammatory demyelinating polyneuropathies. *J Neurol Sci.* 2016;360:170-175.
30. White HD, White BA, Boethel C, et al. Pancoast's syndrome secondary to infectious etiologies: a not so uncommon occurrence. *Am J Med Sci.* 2011;341(4):333-336.
31. Vemuri C, McLaughlin LN, Abuirqeba AA, et al. Clinical presentation and management of arterial thoracic outlet syndrome. *J Vasc Surg.* 2017;65(5):1429-1439.
32. Aralasmak A, Karaali K, Cevikol C, et al. MR imaging findings in brachial plexopathy with thoracic outlet syndrome. *AJNR Am J Neuroradiol.* 2010;31(3):410–417.
33. Akita K, Ibukuro K, Yamaguchi K, et al. The subclavius posticus muscle: a factor in arterial, venous or brachial plexus compression? *Surg Radiol Anat.* 2000;22(2):111-115.
34. Forcada P, Rodríguez-Niedenführ M, Llusá M, et al. Subclavius posticus muscle: supernumerary muscle as a potential cause for thoracic outlet syndrome. *Clin Anat.* 2001;14(1):55-57.
35. Demondion X, Boutry N, Drizenko A, et al. Thoracic outlet: anatomic correlation with MR imaging. *AJR Am J Roentgenol.* 2000;175(2):417-422.